

Vibrational Properties of SnGeS₃ under High Pressure

K. INOUE, V. STERGIOU¹, Y. S. RAPTIS¹ and Z. V. POPOVIĆ^{2,*}

*Institute of Scientific and Industrial Research, Osaka University,
8-1 Mihogaoka, Ibaraki 567-0047*

¹*Physics Department, National Technical University of Athens, GR 157 80 Athens, Greece*

²*Institute of Physics, P.O.Box 68, 11080 Belgrade, Yugoslavia*

(Received June 19, 2000)

We measured Raman spectra of SnGeS₃ single crystal under hydrostatic pressure up to 19.5 GPa. Fourteen of the seventeen modes observed at low pressures disappear around 7 GPa. The remaining three modes persist up to 11.5 GPa. No scattering activity is found above 19.5 GPa. All these changes, as well as color changes, are reversible. The intensities of the Raman modes of SnGeS₃ were calculated using valence-force-field and a bond polarizability model. We have shown that the interchain interaction is responsible for the intensity exchange of 346 cm⁻¹ and 364.5 cm⁻¹ modes under pressure. An assignment to internal and external modes is also proposed.

KEYWORDS: high pressure, Raman spectroscopy, SnGeS₃, valence-force-field and bond-polarisability model

§1. Introduction

Raman scattering of materials at high pressure is one of most effective method for the investigation of forces which bond atoms in crystals. Molecular crystals are characterized by great disparity between intermolecular and intramolecular distances; this feature makes them much more sensitive to the hydrostatic pressure than the three-dimensional network crystals. There are several trends which characterize the Raman spectra of molecular solids under pressure. By pressure application the ratio of inter- to intra-molecular forces increases and consequently the material losses the molecular character. Because of that the intermolecular modes shift to intramolecular frequency region. Since the intermolecular modes are sensitive to pressure, high pressure can help to resolve external (intermolecular, lattice) from internal (intramolecular) modes and/or to resolve near degenerate modes by enhancing their splitting. Further, the molecular crystals attracted a considerable interest because of the pressure-induced amorphization¹⁾ and the polymorphic transitions under pressure.²⁾

SnGeS₃ belongs to the ternary sulfides group of the A^{II}B^{IV}S₃ configuration where A^{II}=(Sn, Pb) and B^{IV}=(Ge, Sn). The crystal structure of A^{II}GeS₃ is monoclinic with four molecules per unit cell (space group P2₁/c).³⁾ The basic building block of SnGeS₃ crystal structure are GeS₄ tetrahedra that are linked via a common corner to form infinite chains along the *c*-axis. The unit cell of SnGeS₃ consists of two such chains that are linked to each other via Sn atoms. The average distance between Ge and S atoms inside a GeS₄ tetrahedra is 0.223 nm. The distances between Sn and S atoms vary from 0.263 nm to 0.2936 nm (average value 0.286 nm).³⁾

Figure 1 shows the schematic representation of SnGeS₃ crystal structure in (bc) and (ab) plane in terms of the coordination tetrahedra.

By applying pressure on SnGeS₃, the GeS₄-chains come closer with a tendency to form a layer. Consequently, the ratio of intra-to-inter-chain force constants decreases and material losses its anisotropy. These structural changes have a strong influence on the phonon dynamics, as we will discuss later.

The vibrational properties of the SnGeS₃ crystal in ambient pressure and low temperatures have been studied through infrared and Raman spectroscopy.⁴⁾ 12A_g + 15B_g Raman active modes have been observed (out of the 30 predicted by factor-group-analysis). These modes are grouped into two spectral ranges: below 250 cm⁻¹ (bond bending vibrations together with external vibrations) and between 340 and 430 cm⁻¹ (bond stretching vibrations). The significant force-constant anisotropy between the intrachain and interchain forces was deduced from the frequency difference of the Raman and infrared Davydov doublets.⁴⁾ Some of our preliminary results are discussed in.⁵⁾

In this paper we have measured Raman spectra of SnGeS₃ single crystals under pressure. We estimated the pressure coefficients for most of Raman modes and identified the 36.6 cm⁻¹ mode as an external one. In the bond stretching region there are two modes at 346 and 364.5 cm⁻¹ which show an intensity exchange in the pressure range 0–7 GPa. By means of calculation of Raman mode intensities, based on valence-force-field and bond polarizability (VFF-BP) model, we concluded that the mode intensity exchange appears due to a change of the force constant difference between the non-bridging (Ge–S) and the bridging (Ge–S–Ge) bonds in the GeS₄-chains. By further pressure increase the Ge–S force constants become isotropic, leading to amorphization. At 19.5 GPa there is no more scattering activity. All pres-

*Present address: Laboratorium voor Vaste-Stoffysica en Magnetisme, K. U. Leuven, Celestijnenlaan 200D, B-3001 Leuven, Belgium.

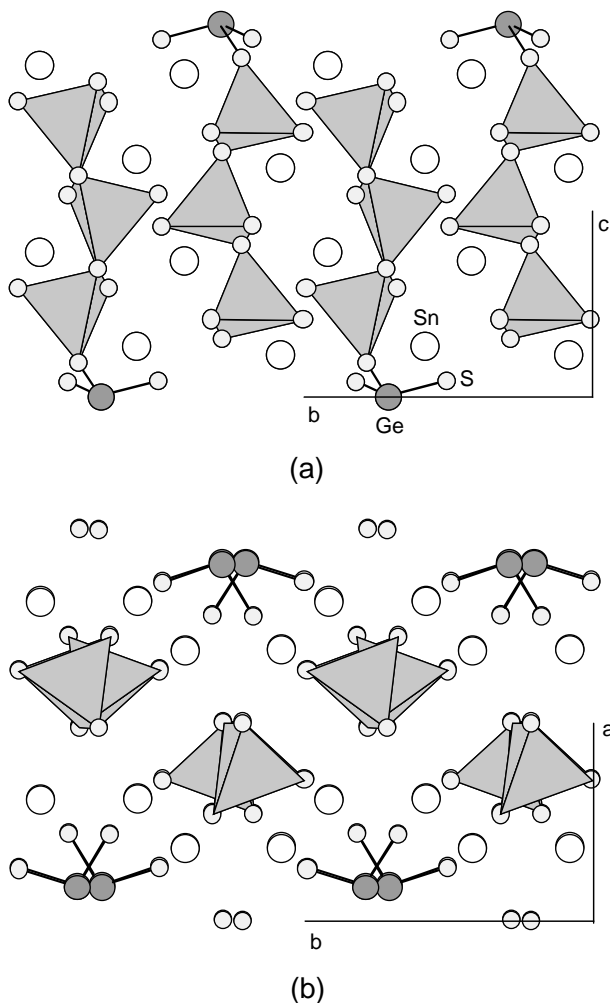


Fig. 1. Schematic illustration of SnGeS₃ crystal structure in (a) (100) and (b) (001) planes.

sure changes are reversible.

§2. Experimental Details

High-pressure Raman scattering measurements were carried out at room temperature, using a gasketed diamond-anvil-cell (DAC).⁶⁾ Single crystals of SnGeS₃ of typical size $50 \times 50 \times 50$ (μm)³ were loaded in the cell, with a 4 : 1 methanol/ethanol mixture as a pressure medium. The standard ruby luminescence was used for pressure calibration. The deviations from the hydrostatic conditions (according to the Ruby line-profiles), above the transition of the pressure medium into glass state at 10.5 GPa, were small enough to be ignored, in accordance with the literature.⁷⁾

Raman spectra were excited with the 568.2 nm Kr⁺ ion laser line, focused on a spot of typical size ≈ 25 μm . The laser power was less than 50 mW. Polarized measurements were not possible due to the polarization scrambling of the incident and the scattered light by the sapphire backing block of the DAC. The scattered light was analyzed with a double (Spex 1403) spectrometer and detected with a cooled photomultiplier. Plasma lines in the vicinity of the excitation line of 568.2 nm were used as independent frequency calibration standards during

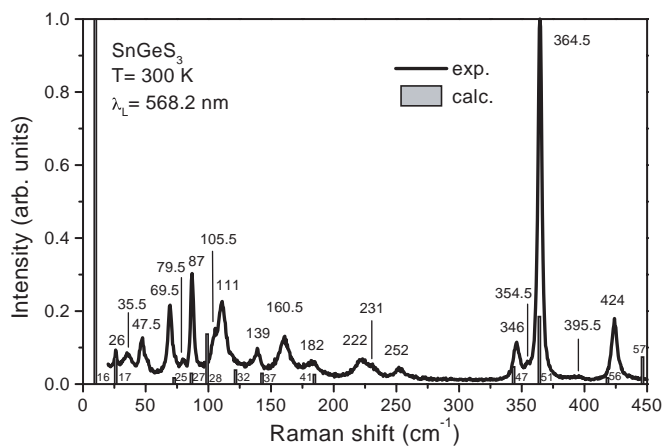


Fig. 2. Unpolarized Raman spectrum (solid line) of SnGeS₃ at room temperature and ambient pressure. Vertical bars represent the intensities of Raman active phonons of A_g symmetry calculated using a VFF-BP model. The calculated phonons are sequentially numbered from low energy mode. The intensities of the calculated modes in the bond stretching region are multiplied by factor 10.

the pressure measurements.

§3. Results

Figure 2 shows an unpolarized Raman spectrum of SnGeS₃ measured at ambient conditions. We observed 17 Raman modes in all. These modes are grouped into a low-(below 260 cm^{-1}) and a high-(between 340 and 430 cm^{-1}) frequency range. The lowest energy peak at 26 cm^{-1} is a laser plasma line. Next peak, as will be discussed further, is an external mode which originate from interchain vibrations. All other modes in the low frequency region are the bond-bending intrachain modes. The frequency gap between 260 cm^{-1} and 340 cm^{-1} divides the bond-bending from the bond-stretching vibration region. Four modes at about 346 , 364.5 , 395 and 424 cm^{-1} are bond stretching vibration modes of the A_g symmetry. Two additional modes, clearly observed at low temperature at 362 and 408 cm^{-1} ,⁴⁾ are of B_{1g} symmetry. These modes are of a very low intensity and it was not possible to extract them from the level of noise in our high pressure measurements. The frequency gap between the bond-bending and the bond-stretching vibrations appears due to difference of force constants between the stretching and bending vibrations.

The Raman spectra of SnGeS₃ for different pressures are shown in Fig. 3. 17 Raman active modes are observed up to moderate pressures (7 GPa). The remaining three modes persist up to 11.5 GPa. Above 19.5 GPa there is no more scattering activity. Upon releasing of the pressure from 19.5 GPa to zero, the ambient condition spectrum is fully recovered, Fig. 3(j).

The most distinctive behavior of the spectra given in Fig. 3 is the gradual change of the relative intensity of the two modes at 346 and 364.5 cm^{-1} , under pressure. We propose (§4.2) that this pressure-dependent intensity change is due to a change in the character of the vibrational motions, which is closely related to level crossing

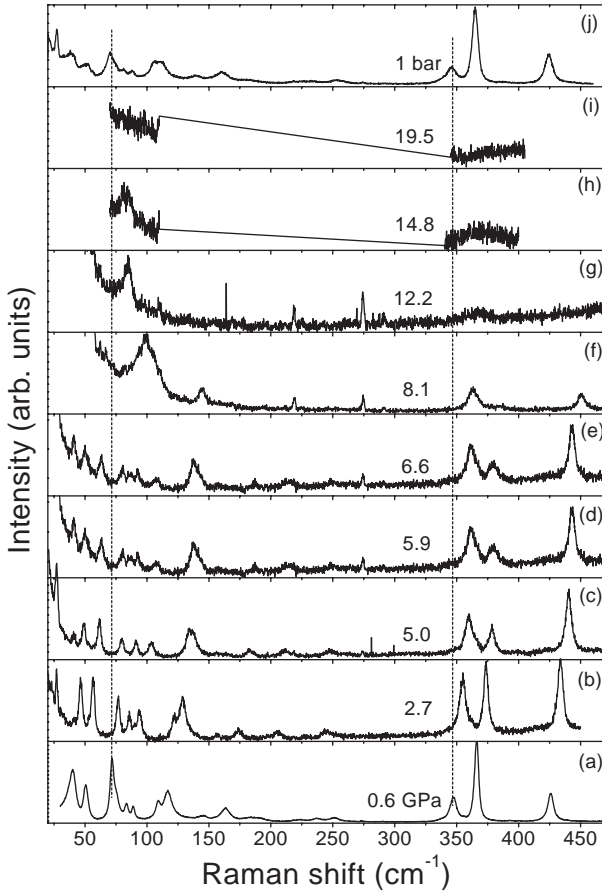


Fig. 3. Raman spectra of SnGeS₃ under pressure. Spectrum at 1 bar (j) is measured after pressure release. Vertical dotted lines are guides for the eyes to check pressure-induced shifts and reversibility.

induced by the pressure.

§4. Discussion

4.1 Pressure coefficients

The effect of pressure on the mode frequencies is illustrated in Fig. 4. The lines represent a polynomial ($\omega = A + B_1p + B_2p^2$) fit. The best fit parameters are given in Table I. There are modes which show a very weak variation of their frequency under pressure. The lowest-lying optical mode at about 40 cm⁻¹ belongs to this group. No frequency shift of this mode with pressure leads us to conclusion that this mode can also be assigned as plasma line (which should appear at about 38 cm⁻¹). In contrast, a mode at 36.6 cm⁻¹ in ambient pressure, shifts to 50 cm⁻¹ when pressure increases to 5 GPa. We assigned this mode as external mode because of its largest pressure coefficient ($B_1/A = 9.1 \times 10^{-2}$ GPa⁻¹, see Table I) and no infrared counterpart, as discussed in.⁴⁾ The other low-frequency modes have lower pressure coefficients and belong to the bond-bending vibrations. No distinguish frequency gap between external (inter-chain) and internal (intrachain) modes does not allow us to assign other external from bond bending (internal) modes. Some of low-frequency modes show a “crossing” or an “anticrossing” behavior under pressure. For in-

Table I. Frequencies and pressure coefficients for some of Raman active modes of SnGeS₃. ω represents the mode frequencies at ambient conditions. B_1 , B_2 and A , are linear, quadratic and free terms of polynomial fit $\omega = A + B_1p + B_2p^2$, respectively.

ω (cm ⁻¹)	A (cm ⁻¹)	B_1 (cm ⁻¹ / GPa)	B_1/A (10 ⁻² / GPa)	B_2 (cm ⁻¹ / GPa ²)
—	40±0.14	0.008±0.002	0.0002	0
35.5	36.6±0.7	3.3±0.3	9.1	-0.17±0.02
47.5	49.0±0.4	5.7±0.3	2.8	-0.11±0.045
69.5	69.5±0.3	2.9±0.2	4.2	-0.22±0.03
79.5	80.3±0.6	3.9±0.5	4.9	-0.28±0.07
87	87.0±0.6	1.85±0.4	2.1	-0.24±0.05
105.5	105.7±0.6	4.3±0.5	4.1	+0.28±0.08
111	112.8±0.7	5.7±0.3	5.0	-0.26±0.03
139	138.7±1.1	10.6±1.7	7.7	-1.42±0.42
160.5	160.1±0.4	4.7±0.4	2.9	-0.05±0.06
182	179.9±0.8	9.0±0.5	5.0	-0.54±0.08
346	346.3±0.6	2.7±0.2	0.79	-0.09±0.02
364.5	364.2±0.5	3.3±0.3	0.90	-0.15±0.04
424	423.7±0.5	3.3±0.2	0.77	-0.04±0.02

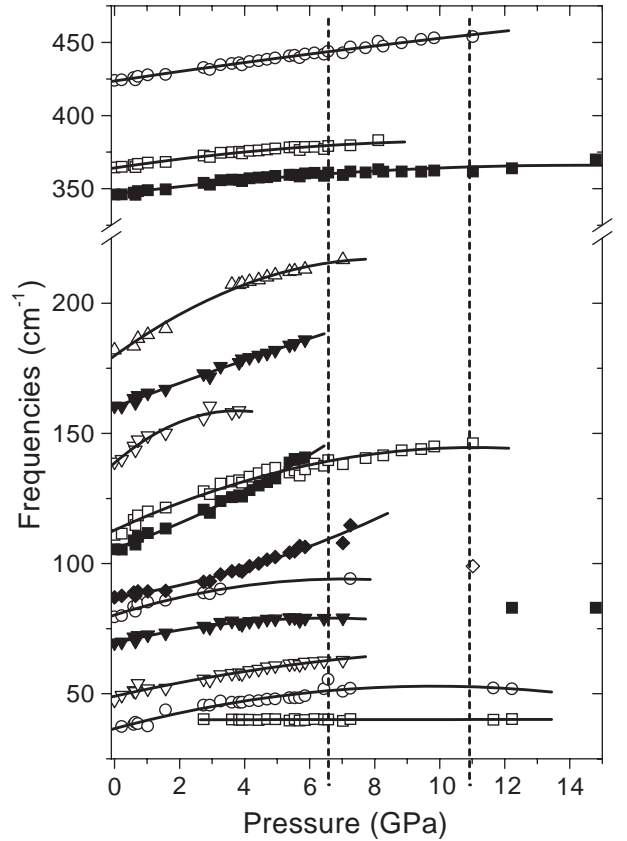


Fig. 4. Pressure dependence of selected Raman mode frequencies of SnGeS₃. Dotted lines mark the three different pressure regions (see text for details). The solid lines are polynomial fit obtained with parameters given in Table I.

stance, the mode pair at 80/87 cm⁻¹ shows an anticrossing at about 2 GPa. On the other hand, the mode pair at 105/112 cm⁻¹ shows a crossing because these modes are of different symmetries (A_g/B_g).²⁾

The three highest frequency modes show reduced pres-

sure coefficient, smaller by one order of magnitude ($\leq 0.9 \times 10^{-2} \text{ GPa}^{-1}$), in comparison to the low-frequency ones. This fact confirms that such modes are assigned to internal bond-stretching vibrations of the GeS₄-chains.

4.2 Crossing of scattering intensity

As we have already mentioned, the most interesting finding in the spectra given in Fig. 3 is the change of intensity of two modes at 346 and 364.5 cm⁻¹ under pressure. To explain this intensity exchange we have used a combined valence-force-field and bond polarizability (VFF-BP) model presented in details in ref. 8. The dynamical matrix of the network structure is described in terms of the sum of bond stretching forces between two atoms and the bond bending forces of two neighboring bonds. Many force parameters can be introduced empirically to obtain good agreement with the experimental results. However, we have limited the number of the parameters to the minimum required to explain the remarkable feature of the two modes at 346 and 364.5 cm⁻¹ as well as the gross spectral features such as the frequency-gap between 260–340 cm⁻¹, see Fig. 2. Thus, instead of the precise fitting between the calculated and the experimental spectra for all vibrational modes, we have concentrated to the role of the essential interactions which are responsible for the exchange of the mode intensity. The model parameters are defined as follows: The bond stretching force constant k_{lt} corresponds to the terminated (non-bridging) Ge–S bonds, while k_{lc} corresponds to the bond stretching force constant along –Ge–S–Ge–S– chains (bridging bond). The two bond bending force constants k_{Ge} and k_{S} correspond to the bending of S–Ge–S and Ge–S–Ge bond configurations, respectively (Fig. 5). Although force constants are pressure dependent, we introduce only one pressure dependent force by a formal parameter $p = (dk_{\text{lt}}/dP - dk_{\text{lc}}/dP)P$, where P is the pressure. This parameter is related to the pressure coefficient difference of the bond stretching forces for the Ge–S bonds in the tetrahedra. The numerical values of the model parameters at ambient pressure (in units of 10⁻¹⁹ J) are $k_{\text{lt}} = 1.76$, $k_{\text{lc}} = 2.3$, $k_{\text{Ge}} = 0.1$, $k_{\text{S}} = 0.05$ (as well as the $k_2 = 3$, $k_3 = 1$ as described below), and are chosen in such a way to reproduce the frequencies and relative intensities of the two modes around 350 cm⁻¹, at ambient conditions. The assumed values (and their relative P -dependence) of k_{lt} and k_{lc} imply that the bond forces are different for terminated and non-terminated bonds in the tetrahedra at ambient pressure, while they approach a common value at high pressures. We numerically assign $dk_{\text{lc}}/dP = 0$ to the formal definition of the p -parameter. Thus, the only P -dependent force constant is the $k_{\text{lt}} = 1.76 + p = 1.76 + (dk_{\text{lt}}/dP)P$. The numerical value for the derivative dk_{lt}/dP is taken equal to 0.043 (10⁻¹⁹ J/GPa). This value gives the best fit for the intensity ratio vs P -dependence of the two peaks under consideration. Under these assumptions, the two different (terminated and non-terminated) Ge–S bonds get the same bond-stretching force-constant around 12.6 GPa. We do not consider the absolute strength of the tetrahedral internal force-constants, but rather their relative P -dependence. This simplification is enough to explain the

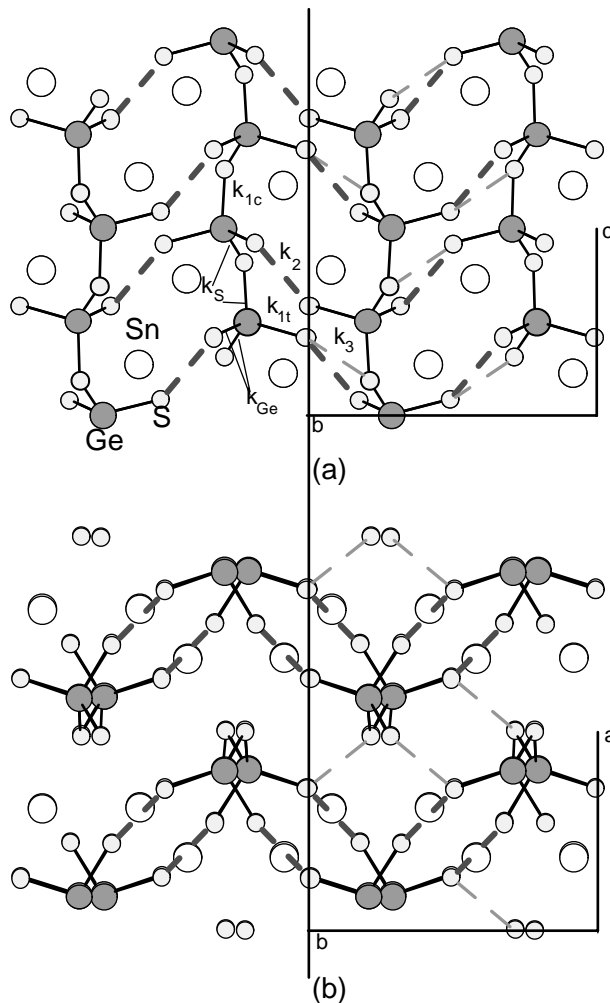


Fig. 5. Projection of SnGeS₃ crystal structure on (a) (100) and (b) (001) plane. The S–S bonds with k_2 and k_3 stretching force constants are represented by dotted and dashed lines, respectively.

intensity changes of the two modes as described below. The Sn atoms, which are located outside the tetrahedra and then regarded as background atoms, are not considered explicitly in the present model, since neighboring Sn–S interactions mainly affect the modes located below the frequency gap (below 260 cm⁻¹) in the calculations.

To calculate the Raman mode intensities we assign an ellipsoidal bond polarizability to each bond, as well as to the lone-pair electrons of the chalcogen atoms (S). The polarizabilities change linearly with the strains ($\delta r_i/r_i$), as described in ref. 8, but their proportionality factors are considered as independent of the pressure within our model. As it is shown later this simple assumption is enough to describe the relative intensity changes of corresponding Raman modes.

Let us first consider the Raman spectra of a GeS₄-chain, the basic building block of the SnGeS₃ crystal structure. Figure 6(a) shows the frequencies and the relative intensities of the Raman modes of an isolated GeS₄-chain at $p = 0$. The lowest frequency mode in the bond-stretching vibration region at about 290 cm⁻¹ represents the A₁ vibration of the GeS₄ tetrahedra, whereas the

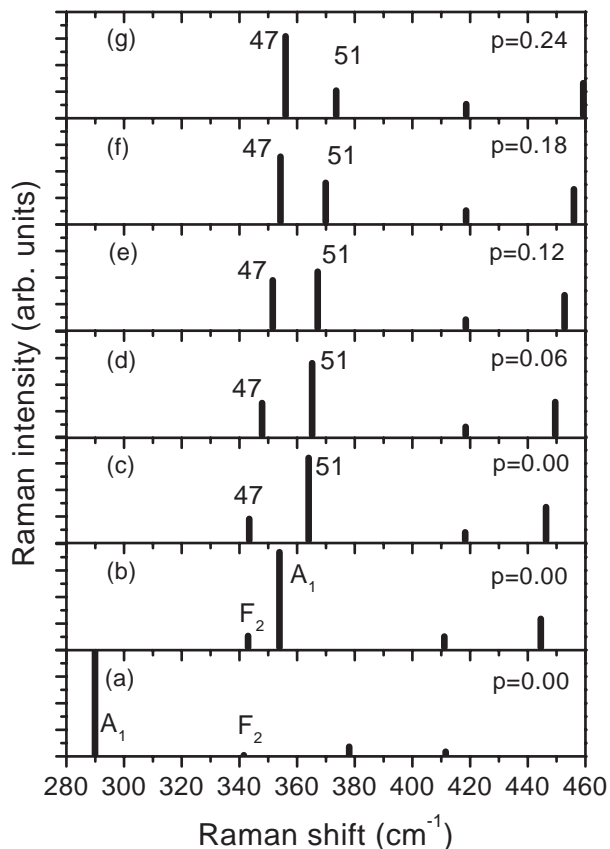


Fig. 6. Raman spectra of SnGeS₃ calculated by a VFF-BP model: (a) isolated chain; (b) calculated spectra by taking into account interchain S–S bonds with k_2 force constant; (c)–(g) spectra calculated with k_2 and k_3 interchain force constants for different values of p -parameter.

higher frequency modes (between 340 and 420 cm^{-1}) are the F_2 vibrations, where A_1 and F_2 denote the symmetries of normal modes of the GeS_4 tetrahedral molecule. Strictly speaking, since the tetrahedra in the chain are connected via an S atom, pure A_1 and F_2 vibrations are no longer normal modes. However, since the angle of Ge–S–Ge bonds (103.5°) is near to the right angle, the coupling between the vibrations of neighboring tetrahedra is somewhat weak and the vibration of the atoms in the chain remains almost similar to that of the isolated GeS_4 molecule. Therefore, we denote them as A_1 -like and F_2 -like modes. The A_1 -like mode has much stronger intensity than F_2 -like ones, see Fig. 6(a). According to the calculation for $p > 0$ (not shown in Fig. 6) the frequencies of all these modes move to higher energies with pressure, without any peculiarity such as crossing, anticrossing, overlapping or intensity exchange. Thus, we concluded that the experimental spectra cannot be explained within the framework of the molecular vibrations of the isolated chains, even with more accurate values of model parameters.

In the next stage we introduced the S–S bonds connecting the chains in the unit cell. This is shown by the dotted lines in Fig. 5. Introducing an S–S bond stretching force $k_2 = 3.0$, results in a shift of the A_1 -like mode to the frequency higher than that of the lower F_2 -like

mode, as shown in Fig. 6(b).

Since the spectrum predicted by the model is still far from the experimental one, we proceed one step further and introduce interchain S–S interactions represented by dashed lines in the right panel of Fig. 5(b). The corresponding bond-stretching force is tentatively assumed as $k_3 = 1.0$. The results of this last modification are shown in Figs. 6(c)–6(g). The comparison between the calculated and the experimental spectra is presented in Fig. 2 for $p = 0$ and in Fig. 7 for different pressures. As it is shown in Fig. 2, an agreement between calculated and experimental spectra is rather poor in the low-frequency region because present model is too simple to fit those modes. However, it should be noted that no significant dependence of those modes on the parameter p is observed in the calculated region of p . This agrees with the experimental results below 7 GPa. In contrast, there is a good agreement between the calculated frequency and intensity of the modes around 350 cm^{-1} and the experimental spectra. The mixing due to the interchain interaction is so strong that both modes can not be labeled as A_1 -like or F_2 -like. Therefore, we denoted them in Fig. 2 by No. 47 and No. 51, the sequential number of calculated modes. The atomic motions of these modes are rather complicated. However, it is possible to describe the motions of Ge and S atoms by a linear combination of the normal modes of the constituent GeS_4 tetrahedra including translation and rotation. The dis-

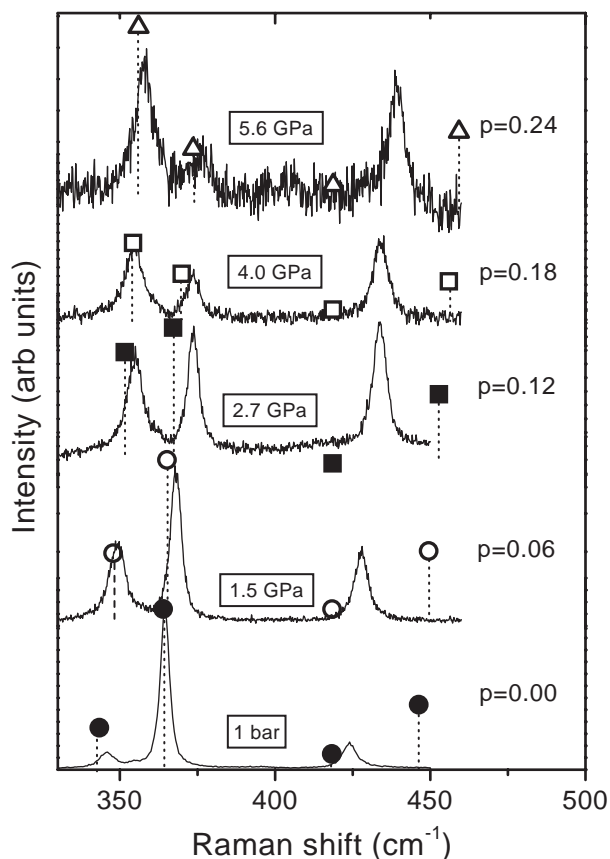


Fig. 7. Raman spectra of SnGeS₃ at several pressures in comparison with VFF-BP model calculated bands, indicated by marks with vertical dashed lines.

placement vector \mathbf{u}_i of the i 'th atom can be expressed by $\mathbf{u}_i = \sum_{\beta} a_{\alpha} \mathbf{u}_{\alpha,i}$, where a_{α} is a numerical coefficient, and \mathbf{u}_{α} is the motion of the tetrahedral normal mode: $\alpha = A_1, E, 2F_2, 3$ rotations and translations. The mode intensity is defined as $I_{\alpha} = a_{\alpha}^2 / \sum_{\beta} a_{\beta}^2$. The mixed character of the two modes around 350 cm^{-1} can be examined by the use of vibrational mode components of the tetrahedra. Namely, the lower frequency mode (no. 47) is made of mainly F_2 -type mode at ambient pressure, and it becomes A_1 -type above $p = 0.2$. The other mode (no. 51) is A_1 -type at ambient conditions, and it changes to F_2 -type above $p = 0.05$. These changes with the pressure are shown in Fig. 8(a). This strong mixing results in a frequency anticrossing of the two modes and a drastic intensity change, as shown in Fig. 8(b), in spite of the assumption of the independence of bond polarizability parameters on pressure.

4.3 Phase transition and amorphization

In the pressure range up to 7 GPa there is no sudden changes of the mode frequencies with pressure, no splitting, and even no appreciable broadening of modes. At the same time, the initially asymmetric bridging and non-bridging Ge-S bonds become more symmetric with pressure. This reduces the crystal anisotropy, operating as a precursor of the pressure-induced amorphization. The same tendency to a common stretching force constant between bridging and non-bridging bonds has been also observed in the case of Ge-O bonds in Li_2GeO_3 .⁹⁾ In our case, the tendency towards similar dynamics between terminating (non-bridging) and non-terminating (bridging) Ge-S bonds leads both to the intensity exchange between two high-frequency modes and to the triggering of the amorphization process.

The mode-broadening combined with an appearance of a new-mode at about 100 cm^{-1} at higher pressures [Fig. 3(f)], can be an indication of structural phase transition. Further pressure increase to 12.2 GPa leads to two broad modes at $\sim 80 \text{ cm}^{-1}$ and $\sim 360 \text{ cm}^{-1}$, Fig. 3(g). The shape and frequency of these modes correspond to that of amorphous GeS_2 .^{10,11)} In this pressure range (7–12 GPa), the long-range order is lost with a subsequent disappearance of the low-frequency modes. The short range order of the GeS_4 tetrahedra is retained up to 19 GPa. It is not clear whether the disappearance of any Raman activity above this pressure is due to a complete amorphization or due to pressure-induced decrease of the energy gap. Further experimental measurements, either X-ray (amorphization) or optical measurements (metalization), are necessary to resolve this problem. Upon the pressure release, the initial spectrum is almost recovered. We have observed only a slight broadening of the low-frequency bands, while the high-frequency ones recover both their relative intensity and FWHM as well.

With reference to the optical properties of the material, the orange color of SnGeS_3 sample at ambient pressure turns to opaque around 11 GPa, in agreement with the red shift of the energy gap of most of semiconducting materials.^{2,12)} The color change reverses upon pressure release, following the general pattern.

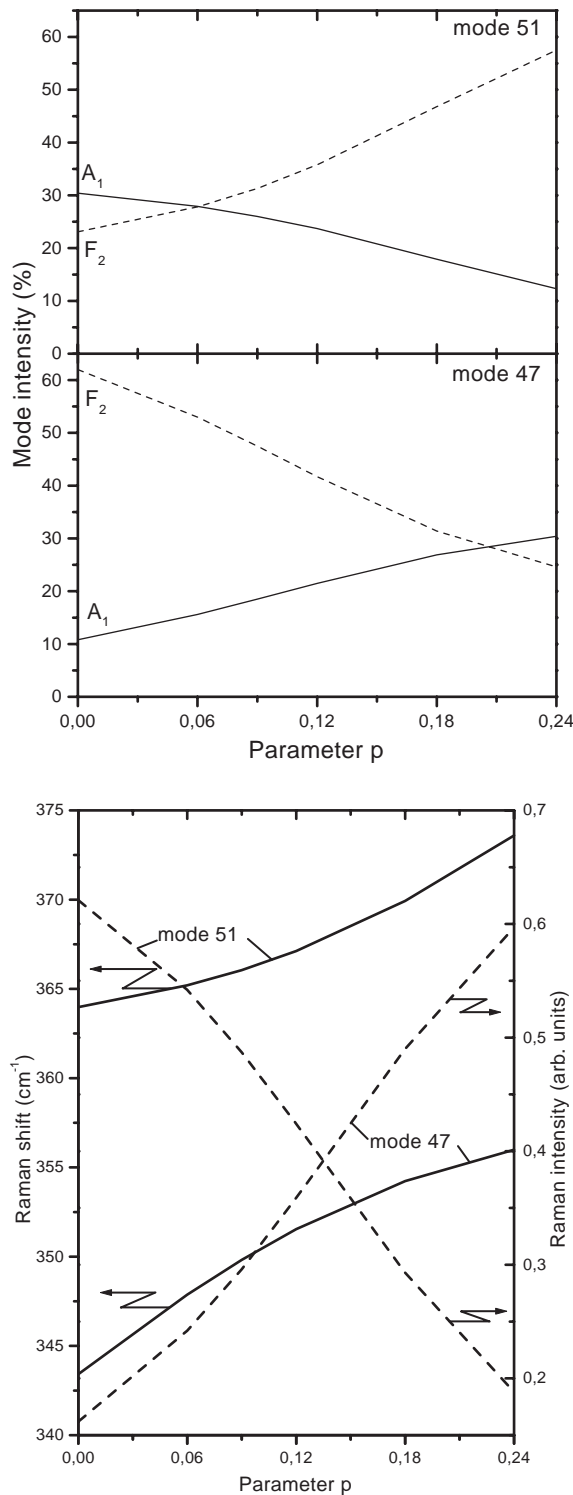


Fig. 8. Pressure dependence of (a) the mixed-type character, (b) the mode-frequencies, and the Raman intensity of the no. 47 and no. 51 modes, calculated by the VFF-BP model.

§5. Conclusion

In conclusion, we have studied the vibrational properties of SnGeS_3 under hydrostatic pressures up to 19.5 GPa. The pressure induced intensity exchange of 346 and 364.5 cm^{-1} modes is explained, as a consequence of the reduction of the inter-to-intra-chain force constants anisotropy, by means of the valence-force-field and bond polarizability model calculations. We

found (i) slight structural modifications due to pure dynamical changes (0–7 GPa), (ii) combined dynamical changes with partial amorphization and energy gap decrease (7–12 GPa), and (iii) pressure induced amorphization (above 12 GPa). The material turns opaque above 11 GPa and it shows no scattering activity above 19.5 GPa. The observed changes are reversed upon pressure release. We estimated the pressure coefficients for most of observed modes also.

Acknowledgments

This work was supported by Serbian Ministry of Science and Technology under Project 01E09, and by National Technical University, Athens. Useful discussions, at the early stage of this work, with the late Prof. E. Anastassakis^(†) are emotionally commemorated. One of the authors (K.I.) is partially supported by a Grant-in-Aid for Scientific Research (C) from the Ministry of Education, Culture, Sports, Science and Technology (Japan).

-
- 1) Z. V. Popović, Z. Jakšić, Y. S. Raptis and E. Anastassakis: *Phys. Rev. B* **57** (1998) 3418.
 - 2) Z. V. Popović, M. Holtz, K. Reiman and K. Syassen: *Phys. Status Solidi B* **198** (1996) 533.
 - 3) M. Ribes, J. Olivier-Fourcade, E. Philippot and M. Maurin: *Acta Crystallogr. Sect. B* **30** (1974) 1391.
 - 4) Z. V. Popović: *Phys. Rev. B* **32** (1985) 2382.
 - 5) V. C. Stergiou, Y. S. Raptis, Z. V. Popović and E. Anastassakis: *High Pressure Res.* **18** (2000) 189.
 - 6) G. Huber, K. Syassen and W. B. Holzapfel: *Phys. Rev. B* **15** (1977) 5123.
 - 7) A. Jayaraman: *Rev. Mod. Phys.* **55** (1983) 65.
 - 8) K. Inoue, O. Matsuda and K. Murase: *Solid State Commun.* **79** (1991) 905.
 - 9) Y. Xu, Y. Li and G. Lan: *Spectrochim. Acta A* **52** (1996) 1417.
 - 10) R. Zallen: *Phys. Rev. B* **9** (1974) 4485; R. Zallen and M. I. Slade: *Phys. Rev. B* **18** (1978) 5775.
 - 11) A. Perakis, I. P. Kotsalas, E. A. Pavlatou and C. Raptis: *Phys. Status Solidi B* **211** (1999) 421.
 - 12) B. A. Weinstein, R. Zallen, M. L. Slade and J. C. Mikkelsen: *Phys. Rev. B* **25** (1982) 781.
-